BULLETIN OF THE POLISH ACADEMY OF SCIENCES
TECHNICAL SCIENCES,
DOI: 10.24425/bpasts.2025.155895

An approximate analytical solution of the gear meshing problem based on MSM using DynPy Python library

Krzysztof Twardoch[12]*, Krzysztof Kaczmarzyk[2], Grzegorz Długopolski[2], Bogumił Chiliński[12]

[1]Division of Numerical Methods and Intelligent Structures, [2]Faculty of Automotive and Construction Machinery Engineering, Warsaw University of Technology, Poland

Abstract.
The paper presents the mathematical and numerical analysis of a 1-DOF (one-degree-of-freedom) dynamic model of the helical gear with Time-Varying Mesh Stiffness (TVMS). The article aims to determine an analytical solution for the presented model using a proprietary computational environment and to verify the results with numerical simulations and other solutions available in the literature. The paper presents the determination of a 2-DOF (two-degree-of-freedom) dynamic model and its reduction to a 1-DOF model. The concept of the created environment, the applied libraries, and the application basics are discussed. Based on the work effects, an analytical solution using the Multiple Scales Method (MSM) was found and positively verified. The article presents the convergence of the obtained results and the added value as an analytical solution. This confirms the effectiveness of the novelty approach, which provides a framework that bridges the gap between directly determining a solution and manual calculations. It should be noted that time complexity is especially important for performance computing. Observations suggest significant advantages to using an analytical solution due to its precision and relatively low computational cost. Although obtaining an analytical solution is more time-consuming, it reduces the possibility of errors with numerical methods.

Key words: gear meshing, parametric vibrations, Time-Varying Mesh Stiffness (TVMS), Multiple Scales Method (MSM), analytical modeling, numerical simulations, drive system, gear dynamics

1. INTRODUCTION

There is growing interest in sophisticated computational methods for gears commonly used in industry [1], [2]. This is related to the demand for increasingly heavy-duty constructions. This is dictated by considerations of energy savings, i.e. reducing the energy intensity of machinery and equipment. Thus, the current trend in the design of gear is characterized by a desire to minimize dimensions and weight. There is a direct proportional relationship between energy savings and design strain. This trend implies a change in the frequency structure of the system (a change in eigenfrequencies) due to a change in the basic dynamic parameters of gear such as mass and stiffness. The demand for optimization of mass is associated with a non-unknown impact on the dynamics of the system. Clearly, changing the parameters of the system results in a completely different dynamic response.

In connection with the outlined problem of gear design, a demand arises for precise computational methods based on the determination of analytical solutions [3], [4], [5]. Analytical methods are particularly interesting from the point of view of the optimization process because they provide an explicit mathematical description of the system in the form of clear formulas. This is conducive to the creation of software implementations, enables fast calculations, and obtaining results for different input data, i.e. for different values of system parameters.

One of the important exploratory problems of gears is the possibility of parametric resonance. The main reason for the occurrence of this resonance phenomenon (parametric resonance) is the time-varying stiffness of the mesh, which is due to the essence of the operation of gears, i.e. the meshing of mating wheels and the associated periodically varying number of pairs of teeth that are in the pinion at a given time instant.

This article aims to provide advanced calculational environment and to analyze the parametric vibration of a helical gear system with Time-Varying Mesh Stiffness (TVMS) using the Multiple Scales Method (MSM) and numerical methods within this environment. This study considered a 2-DOF model of the helical gear system. Then, it was reduced to a 1-DOF system to find an analytical solution, evaluate its adequacy, and analyze the phenomenon of parametric vibrations generated in the mesh. The 2-DOF model served as a reference model. In turn, the 1-DOF model served as the basis for determining analytical solutions.

The characteristic of a good model is conciseness (appropriate level of abstraction) and not size (over-expansion). Therefore, one of this work's goal is to propose a simple dynamic model of a helical gearbox and to check whether it corresponds to the physical operating parameters of such a gearbox. The intention is a qualitative analysis. The authors have assumed that considering the problem at this stage of the work will not focus on the exact selection of the system parameters and the possibility of their physical realisation. According to the concept adopted, the proposed approach allows, with the assumed error, to determine analytically the system's dynamic characteristics, without knowledge of numerical data - no numerical

*e-mail: krzysztof.twardoch@pw.edu.pl

simulations are necessary.

The following milestones were defined based on the analysis of the set work objective and the issues to be addressed:

1. Development of an environment supporting analytical calculations, providing tools to support activities at each stage of the calculations.
2. Determination of an analytical solution in the developed environment and verification with other publications.
3. Perform numerical simulations in the created environment for the normative engagement model and for the MSM to verify the effectiveness of the created framework.
4. Compare the forces for different engagement models to select the most accurate (adequate) model.

The realization of the thesis objective fills the gap between the automatic execution of calculations in CAS systems (black box model) and a full understanding of the MSM and manual execution of calculations step by step. This is the added value of the thesis and its novelty.

A comparative analysis of the analytical and numerical model was assumed to assess the proposed methodology's effectiveness within prepare framework and developed by Authors DynPy library. Based on the verified analytical solution, a series of simulations can be performed to analyze the problem under consideration thoroughly. A mathematical model is established describing the relationships between the key parameters affecting the occurrence of parametric resonance of the gearbox. The mathematical conditions for the occurrence of parametric resonance are confirmed as the solution obtained by Multiple Scales Method (MSM).

As already noted (4th paragraph), a good model is characterised by conciseness (an appropriate level of abstraction) rather than size (excessive complexity) to capture the essence of a specific dynamic phenomenon, as exemplified by studies [6], [7], and [8]. Notwithstanding that the considered model is relatively simple and current computing capabilities allow for solving more complex problems, this approach offers certain advantages, allowing for:

- Verify the correctness of the proposed solution (environment, methodology and mathematical dependencies) by analysis and comparison with publications on a similar topic, for example [6], [7], [9].
- Easier understanding of the phenomenon essence of intertooth dynamics — considerations focus only on meshing vibrations, such as references [8], [10].
- Complementary knowledge of the phenomena involved is essential for the efficient analysis of more complex systems, which is why this approach allows for a better understanding of the problem under consideration, thereby enhancing our understanding of real-world systems.

Mathematical modeling has been used for many years. Various mathematical models have recently been created for numerous applications [10], [11]. The flagship research article [12] presents a classic overview of such models. This paper discusses typically used mathematical models and provides a general classification of them. The research focused on the dynamics of helical gears very often refers to the nature of their operation related to the generation of parametric vibrations associated with the time-varying number of pairs of teeth in contact, i.e. in the line-of-action. An interesting example of parametric vibrations and instabilities of an elliptical gear pair research is presented in [13]. The publication evaluates the influence of basic parameters on solution stability. The research used a model to consider factors such as eccentricity or varying mesh stiffness. These effects caused vibrations in the system, which led to the determination of different combination resonances. The calculation results show the coupling effect between the selected frequencies. The authors show that the coupling effect results from the simultaneous occurrence of load, time-varying mesh stiffness, and eccentricity. Studies comparing elliptical and circular gears have unveiled lower vibration amplitudes in elliptical gears, exploring the intricate interactions between eccentricity, stiffness, and load that lead to vibrations and instability in these gear configurations [13]. It is imperative to determine the ranges of irregular gear behaviour, as this may cause chaotic phenomena. This is demonstrated by a numerical investigation on gear dynamics [6]. It presents simulation studies based on a non-linear mathematical model of a gear transmission that considers variable mesh stiffness and backlash, which made it possible to identify areas where the analysed system behaved chaotically. This is illustrated as a frequency spectrum, a bifurcation diagram, a Lyapunov exponent, and a Poincaré map (section).

The interesting field of investigation uder the gears is its modelling and experimental testing [3], [4], [5], [7], [9], [14], [15], [16]. Noteworthy is a publication [17], where the subject of analysis was a helical gear system. A system of shafts, bearings, and disks representing gears was used for modeling. Gears are part of the parametrically excited system because of time-varying mesh stiffness. This study proposed a matrix with harmonic frequencies representing parametrically excited vibration transfer functions. The nonlinear equation of motion for gears was linearized to an equation with the excitation of harmonic frequencies. The proposed transfer matrix can easily show the contribution of the harmonic components. The research follows on from that presented in the papers [18], and [19]. Article [18] presents the analysis of a simplified model. The results obtained were used to analyze gearbox vibrations under axial load. The model includes a shaft, gear system, and housing. In addition, mesh stiffness and a solution to the equation of motion were used to determine the axial force. The relationship between strain and load is used for this purpose. The noise generated by helical gears is also a problem that requires analysis. One research direction is the use of simplified systems subjected to axial load. Models consisting of shafts, bearings, and helical gears are used for this purpose [19].

Although countless dynamic models have been developed, solutions based on numerical methods are predominantly used. Studies presenting analytical solutions are much rarer. Among such studies are those presented in publication [20]. The article presents the system's physical (mechanical) model and

the derivation of the equations of motion. On this basis, the authors analytically determined linear solutions, constituting a mathematical description of vibrations. Furthermore, the publication compares the results of a numerical solution determined from nonlinear equations. It proposes various effects, such as time-varying mesh stiffness, gear profile error, equivalent error, and the influence of static load.

Research has increasingly shifted focus towards a more accurate understanding of gear dynamics by incorporating time-varying mesh stiffness. Departing from traditional quasi-static approaches, these investigations highlight the significance of nonlinear relationships between mesh stiffness and dynamic forces, particularly in spur gear systems analyzed in [8]. An interesting example is also presented in article [21], which concerns dynamic modelling of a harmonic drive in a gear transmission system, considering non-linear changes in stiffness and damping. This contributes to expanding knowledge about torsional vibrations occurring in this type of power transmission system.

Research based on dynamic models is becoming increasingly important in the development of vibroacoustic diagnostic methods for gears, which are commonly used components in power transmission systems [22], [23], [24], [25]. Early identification of degradation processes is essential for planning inspections and repairs, and thus for improving the reliability of all kinematic chain elements. Simulation and experimental studies presented in paper [26] have shown that the use of an identified dynamic model of a gear in a power transmission system allows reliable diagnostic relationships to be obtained for a reliable condition assessment. It is worth noting that, based on simulations and experimental studies, the authors have developed a set of neural network classifiers for diagnosing the type and severity of gear damage with a validation error of less than 5%. It should also be emphasised that condition monitoring is particularly important for preventing unplanned outages in high-value rotating machinery used in power engineering and mining [25], as well as in aerospace. In this regard, advanced and sophisticated diagnostic techniques have been developed by researchers and experts. For example, enhancing gearbox vibration signals by combining a whitening procedure and a synchronous processing method [27] or variational mode decomposition and a convolutional neural network for gearbox fault identification [28].

Expanding the scope of analysis, research has explored the influence of additional degrees of freedom in gear systems, revealing diverse behaviors in non-linear vibration, as presented in [29]. This expanded analysis has proven instrumental in uncovering nuanced aspects of gear dynamics. For instance, to reveal failure mechanisms and investigate local damage in gear systems, the authors of article [22] proposed a 24-DOF dynamic coupling model that considers shafts, bearings and gears. This model can simulate local defects in various locations and provide data and a modelling method for diagnostics.

An article undoubtedly worthy of attention is the work of [30]. The issue of vibrations in a spur gear was analyzed. The article presents considerations on a single-degree-of-freedom (SDOF) linear system in which manufacturing errors and gear stiffness described by a parabolic relationship are considered, which is an effective approach to this issue. The authors used spectral methods and Green's function to determine the system's steady-state vibrations. Based on this, the calculated eigenvalues could assess the system's stability. It should be emphasized that the proposed technique can also be used to solve the problem of a complex description of the varying mesh stiffness. Furthermore, the results obtained were verified using the Floquet method, and stability maps were created. Finally, the results obtained were compared with a numerical solution, which showed a very high level of compliance for all cases considered. Sophisticated models examining time-dependent mesh stiffnesses in planetary gear trains have provided valuable insights into dynamic tooth loads, as shown in [13], [31], [32], [33], [34]. The publications described show an analytical approach where calculations are performed manually, or computational scripts are used as a direct equivalent of manual calculations (only valid for the case under consideration). This indicates a lack of dedicated tools to support this type of computation in the general case.

Although there is no shortage of research on dynamic models of helical gears that focuses on finding analytical solutions, there is still an insufficient number of such studies, and they do not cover all issues. In this paper, the authors have addressed the issue and aim to demonstrate the effectiveness and highlight the advantages of analytical over numerical methods when analysing the dynamics of gears. The aim is to confirm the effectiveness of the analytical approach and the cost-effectiveness of its use in terms of time complexity. Particular focus is given to computation time.

The practical aspects of the proposed methodology for an approximate analytical solution of the gear meshing problem based on MSM can be highlighted as follows:

- The meshing force (inter-tooth force) has a significant impact on gear vibrations, and the mathematical model allows for a better understanding of the vibration response structure.
- This can be used in practice to better determine dynamic surpluses for more accurate gear calculations (reducing iterations in the gear pair design process).
- In addition, an interesting area of application is gear diagnostics, where knowledge of the vibration structure is a key factor for effective fault and defect detection.

The established dynamic model, as well as an analytical approach, may provide a theoretical basis for the fault diagnostics of gear transmission systems, according to recent findings [22].

2. DYNAMIC MODEL OF HELICAL GEAR

The analysis of the gear mesh dynamics requires numerical computations and simulation investigation. Table 1 lists the parameters of the helical gear used in this study.

The gear's dynamic model (Fig. 1) represents an isolated system oriented on the internal factors influencing its vibration behavior. This model includes only two interacting gears, each characterised by base radii r_{bi} and mass moments of inertia J_i (i=1 for the pinion, i=2 for the gear). The pinion is subjected to

[H]

Table 1. Basic parameters of helical gear

	Symbol	Value	Unit
Number of teeth of the pinion	z_1	26	-
Number of teeth of the gear	z_2	53	-
Module (gear system parameter)	m_n	2	mm
Center distance of the pinion	d_1	52	mm
Center distance of the gear	d_2	106	mm
Gear ratio	u	2.04	-
Pressure angle	α_{wt}	20	°
Pitch diameter of the pinion	d_{b1}	48.864	mm
Pitch diameter of the gear	d_{b2}	99.607	mm
Face width ratio	ε_α	1.412	-
Length of the contact line	g_α	8.338	mm
Rotational speed of the pinion	n_1	1460	rpm
Input torque	T_1	98.12	Nm

a constant input torque T_1, while the gear is subjected to an output torque T_2. Two parallelly connected elements with elastic-damping characteristics represent the interaction between the gears, depicting time-varying mesh stiffness $k_m(t)$ and variable damping $c_m(t)$. The proposed dynamic model of the helical gear includes two-degrees-of-freedom ($\phi_1(t)$ and $\phi_2(t)$), corresponding to the pinion and gear rotational motion.

The gear system can be simplified to a single equivalent body with a mass m_{red} (Fig. 2). In this case, the equivalent system undergoes a translational oscillatory motion along the x-axis, and an equivalent force F replaces (consolidates) the torques. This operation is possible because the kinematic properties of gear meshing under investigation are only within the scope of interest. The introduction of the relative generalised coordinate allows the model to be reduced to a single-degree-of-freedom (SDOF).

Kinetic energy of the system is following:

$$T = \frac{J_1\dot{\phi}_1^2}{2} + \frac{J_2\dot{\phi}_2^2}{2} \tag{1}$$

Potential energy of the system is following:

$$V = \frac{k\left(-r_1\phi_1 + r_2\phi_2\right)^2}{2} \tag{2}$$

Dissipative function of the system is following:

$$D = \frac{c\left(r_1\dot{\phi}_1 - r_2\dot{\phi}_2\right)^2}{2} \tag{3}$$

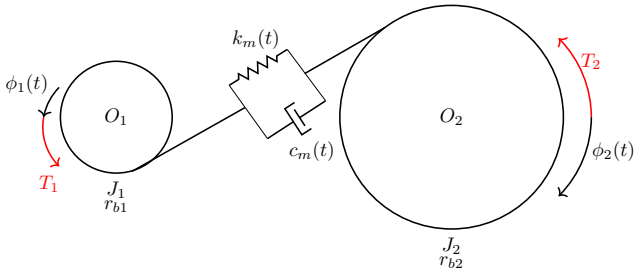

Fig. 1. Dynamic model of the single-stage helical gear as a 2-DOF isolated model

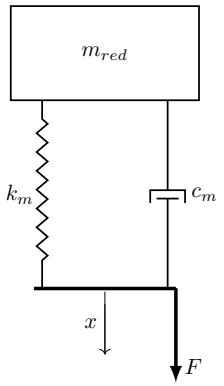

Fig. 2. Dynamic model of a single-stage helical gear as a 1-DOF reduced model

Lagrangian of the system:

$$L = \frac{J_1\dot{\phi}_1^2}{2} + \frac{J_2\dot{\phi}_2^2}{2} - \frac{k\left(-r_1\phi_1 + r_2\phi_2\right)^2}{2} \tag{4}$$

Partial derivatives:

$$\frac{\partial T}{\partial \dot{\phi}_1} = J_1\dot{\phi}_1 \tag{5}$$

$$\frac{d}{dt}\frac{\partial T}{\partial \dot{\phi}_1} = J_1\ddot{\phi}_1 \tag{6}$$

$$\frac{\partial T}{\partial \phi_1} = 0 \tag{7}$$

$$\frac{\partial V}{\partial \phi_1} = -kr_1\left(-r_1\phi_1 + r_2\phi_2\right) \tag{8}$$

The equation for the second coordinate is as follows:

$$\frac{\partial T}{\partial \dot{\phi}_2} = J_2\dot{\phi}_2 \tag{9}$$

$$\frac{d}{dt}\frac{\partial T}{\partial \dot{\phi}_2} = J_2\ddot{\phi}_2 \tag{10}$$

$$\frac{\partial T}{\partial \phi_2} = 0 \tag{11}$$

$$\frac{\partial V}{\partial \phi_2} = kr_2\left(-r_1\phi_1 + r_2\phi_2\right) \tag{12}$$

The Euler-Lagrange formula can be written in the following form:

$$\frac{\partial V}{\partial \phi_1} + \frac{d}{dt}\frac{\partial T}{\partial \dot{\phi}_1} - \frac{\partial T}{\partial \phi_1} = Q \tag{13}$$

Described calculations result in equations of motion of the system. The motion of the analyzed model (Fig. 1) is described by two differential equations:

$$J_1\ddot{\phi}_1 + r_{b1}c_m\dot{x} + r_{b1}k_m x = T_1 \tag{14}$$

$$J_2\ddot{\phi}_2 - r_{b2}c_m\dot{x} - r_{b2}k_m x = -T_2 \tag{15}$$

where relative displacement along the pressure line is equal to:

$$x = r_{b1}\phi_1 - r_{b2}\phi_2 \tag{16}$$

and relative velocity along the pressure line is given by a formula:

$$\dot{x} = r_{b1}\dot{\phi}_1 - r_{b2}\dot{\phi}_2 \tag{17}$$

Subtracting equations (14) and (15)

$$J_1\ddot{\phi}_1 - J_2\ddot{\phi}_2 + r_{b1}c_m\dot{x} + r_{b1}k_m x + r_{b2}c_m\dot{x} + r_{b2}k_m x = T_1 + T_2 \tag{18}$$

where:

J_1 - mass moment of inertia of the pinion;
T_1 - input torque;
J_2 - mass moment of inertia of the gear;
$\ddot{\phi}_2$ - angular velocity assosiated with the rotational motion of the gear wheels;
$\dot{x}$ - velocity;
k_m - time-varying mesh stiffness;
$\ddot{\phi}_1$ - angular acceleration assosiated with the rotational motion of the gear wheels;
ϕ_1 - first degree of freedom assosiated with the rotational motion of the gear wheels;
c_m - variable damping;
t - time;
ϕ_2 - second degree of freedom assosiated with the rotational motion of the gear wheels;
r_{b1} - pinion radius;
x - imaginary coordinate x;
T_2 - output torque;
r_{b2} - gear radius.

The main result of the presented calculations is the equations of the system's dynamics expressed by a system of second-order differential equations. Appropriate transformations allow the system to be replaced by a single equation, the solution of which represents the motion of the helical gear system.

3. MESH STIFFNESS

The investigated problem was solved by creating a computing environment in Python. For this purpose, the DynPy programming library and the Jupyter tool were used. The DynPy Python library [35] is an object-oriented tool that provides a modular approach to physical phenomena, mainly broadly understood dynamics. DynPy is developed and maintained by the authors of articles [36], [37], and [38]. It finds many different research applications, e.g., in works [39], [40], and [41]. Jupyter Notebook is a popular runtime environment for various scripts or macros written in scripting programming languages like Python or R. The basis is a dynamic system, and key elements are presented in the following listing. For the system to work properly, it is enough to define variables in the `__init__` method and specify physical components in the `components` method.

```
class EquivalentGearModel(ComposedSystem):

    def __init__(self,
                 m=None,
                 k=None,
                 F=None,
                 z=None,
                 c=None,
                 T=None,
                 ivar=None,
                 k_var=None,
                 eps=None,
                 c_var=None,
                 f=None,
                 **kwargs):

        if k_var is not None: self.k_var = k_var
        if eps is not None: self.eps = eps
        if m is not None: self.m = m
        if k is not None: self.k = k
        if F is not None: self.F = F
        if z is not None: self.z = z
        if c is not None: self.c= c
        if T is not None: self.T= T
        if c_var is not None: self.c_var = c_var
        if ivar is not None: self.ivar = ivar
        if f is not None: self.f=f


        self.qs = [self.z]
        self._init_from_components(**kwargs)


    def components(self):

        components = {}
        self.c_var = self.c*(1+0*self.eps*self.
    k_var )
        stiffness = self.k*(1+self.eps*self.
    k_var  )


        self.gear_inertia = MaterialPoint(self.m
    , self.z, qs=self.qs)
        self.gear_stiffness = Spring(stiffness,
    self.z, qs=self.qs)
        self.force = Force(self.F, self.z, qs=
    self.qs)
        self.gear_damping = Damper(self.c_var,
    self.z, qs=self.qs)

        components['gear_inertia'] = self.
    gear_inertia
        components['gear_stiffness'] = self.
    gear_stiffness
        components['force'] = self.force
        components['gear_damping']=self.
    gear_damping


        return components

%
```

The implemented dynamic system allows for a very effective analysis of the system's dynamics. This type of implementation is a scalable and efficient solution. It allows for quick determination of the equations of motion or basic dynamic characteristics as follows:

```
gear_dsys = EquivalentGearModel()
eom_gear=gear_dsys.eoms

display(eom_gear.as_eq_list()[0])

    %
```

The result is an equation displayed in a clear mathematical notation representing this object. This functionality has been achieved by using elements from the SymPy library [42] as a symbolic calculation engine (back-end).

$$-F + c_g\dot{z} + m_{eq}\ddot{z} + k_g\left(\kappa_{mesh}\varepsilon + 1\right)z = 0 \tag{19}$$

where:

κ_{mesh} - formula representing stiffness variation (Fourier expansion of rectangular signal);
c_g - mesh damping coefficient;
m_{eq} - equivalent mass;
k_g - mesh stiffness coefficient;
ε - small parameter;
z - gear vibration displacement;
$\dot{z}$ - gear vibration velocity;
$\ddot{z}$ - gear vibration acceleration;
F - excitation force.

Another method (only implemented within the `class EquivalentGearModel` - local interface) allows for the determination of various stiffness models. Any number of models can be defined. The listing shows a model selection with the key `waves`.

```
gear_dsys = EquivalentGearModel()
stiff_models = gear_dsys._stiffness_models()

display(stiff_models['waves'])  # reference
    model (HA)
display(stiff_models['rect'])   # rectangular
    model (RA)
display(stiff_models['approx']) # Fourier
    approximation (FA)

    %
```

All models considered have the following form:

$$\kappa_{mesh} = -0.5 + 2.5\,\mathrm{sign}\left(\sin\left(\frac{2\pi t}{T}\right)\right) + 1.0\sin\left(\frac{2\pi t}{T}\right)\mathrm{sign}\left(\sin\left(\frac{2\pi t}{T}\right)\right) \tag{20}$$

$$\kappa_{mesh} = 2.5\,\mathrm{sign}\left(\sin\left(\frac{2\pi t}{T}\right)\right) \tag{21}$$

$$\begin{aligned}\kappa_{mesh} = {} & 0.21\sin\left(\frac{30\pi t}{T}\right) + 0.17\sin\left(\frac{38\pi t}{T}\right) \\ & + 0.29\sin\left(\frac{22\pi t}{T}\right) + 0.64\sin\left(\frac{10\pi t}{T}\right) \\ & + 0.46\sin\left(\frac{14\pi t}{T}\right) + 1.1\sin\left(\frac{6\pi t}{T}\right) \\ & + 0.35\sin\left(\frac{18\pi t}{T}\right) + 0.19\sin\left(\frac{34\pi t}{T}\right) \\ & + 3.2\sin\left(\frac{2\pi t}{T}\right) + 0.24\sin\left(\frac{26\pi t}{T}\right)\end{aligned} \tag{22}$$

The mathematical dependencies 20-22 form the basis of the simulations presented. They were selected as example dependencies describing the variability of TVMS (Time-Varying Mesh Stiffness). Equations are presented in the form of the plot visible in Figure 3.

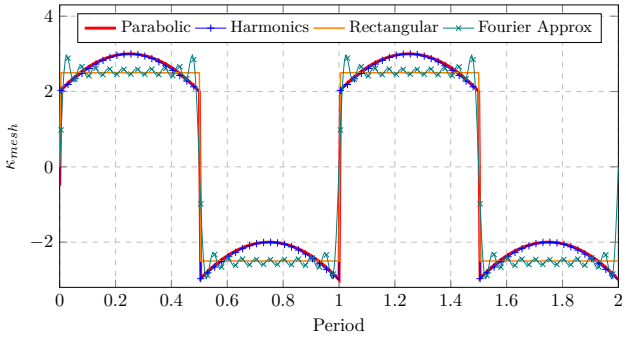

Fig. 3. Mesh stiffness models

Figure 3 compares the various mesh stiffness models used in the simulation studies.

- Parabolic Reference Approximation (PRA) - a mesh stiffness model where the course is a typical approximation pattern using a parabolic function.
- Harmonics Approximation (HA) - a mesh stiffness model based on a periodic function as a quasi-parabolic approximation: considered an adequate matching of the mesh stiffness course pattern.
- Rectangular Approximation (RA) - a mesh stiffness model based on a rectangular approximation: considered a less suitable and lower accuracy matching of the mesh stiffness course pattern compared to harmonic approximation.
- Fourier Approximation (FA) - a mesh stiffness model as an approximation of the mesh stiffness course pattern also proposed in this study: sufficiently good due to frequency response for simulation studies (see study [37]).

Trigonometric functions are necessary for the proposed models' application in MSM. The Fourier series expansion can be determined to obtain an expression containing only `sin` and `cos` functions for each periodic function. The formulas for the series expansion are as follows:

$$k_p = \frac{a_0}{2} + \sum_{n=1}^{\infty}\left(a_n\cos\left(\frac{\pi n k_p}{T}\right) + b_n\sin\left(\frac{\pi n k_p}{T}\right)\right) \tag{23}$$

where:

$$a_0 = \frac{\int_{-T}^{T} k_p \, dt}{T} \tag{24}$$

$$a_n = \frac{2 \int_{-T}^{T} k_p \cos\left(\frac{\pi n t}{T}\right) dt}{T} \tag{25}$$

$$b_n = \frac{2 \int_{-T}^{T} k_p \sin\left(\frac{\pi n t}{T}\right) dt}{T} \tag{26}$$

The results obtained do not contain odd components. The dependencies considered represent the variability of stiffness over time, which allows for a simplification of the analysis. The period is a variable parameter, therefore the analysis is carried out in the period domain. Numerical transformation algorithms for the frequency domain available in the DynPy library were used. It can be concluded that any periodic model can be simplified in this way to an analytical form. The proposed approach allows for assessing the convergence of different models - easy to add when creating a dynamic system.

Based on the study presented in paper [37], all computations were performed for the helical gear parameters listed in Table 1. Equation (19) was used as a base for numerical analysis of the adopted stiffness models (Fig. 3). A series of analyses was carried out. The investigation's results are presented in Figures 4 and 5 (as subplots).

Figures 4 and 5 compare the simulation results obtained for different approximations of mesh stiffness: harmonic (HA), rectangular (RA), and Fourier (FA) approximation. The simulations have been performed for the same period to eliminate uncertainties regarding the frequency of the signals and to enable a direct comparison of courses' shapes and amplitudes. It can be observed that the courses' amplitudes appropriate for single-tooth and double-teeth meshing are similar, but the differences in the courses' shapes are clear. It's worth noting that the FA approximation additionally contains signal modulation, which increases the amount of information transferred.

The parabolic model, widely recognized in the literature as a classical representation of mesh stiffness, is considered a reliable mathematical depiction of actual stiffness behavior along the path of contact. Its accuracy in scholarly discussions is well-established. The HA model serves as a close approximation to the parabolic model and demonstrates high accuracy. On the other hand, the displacement characteristics generated by the HA model are approximate those observed in the parabolic model within the time domain. In contrast, the RA and FA models exhibit certain limitations due to additional simplifications. These models exclude the parabolic segments observed in the time-domain representation, as clearly illustrated in Figure 5, but still sufficiently represent the fundamental gear meshing phenomena.

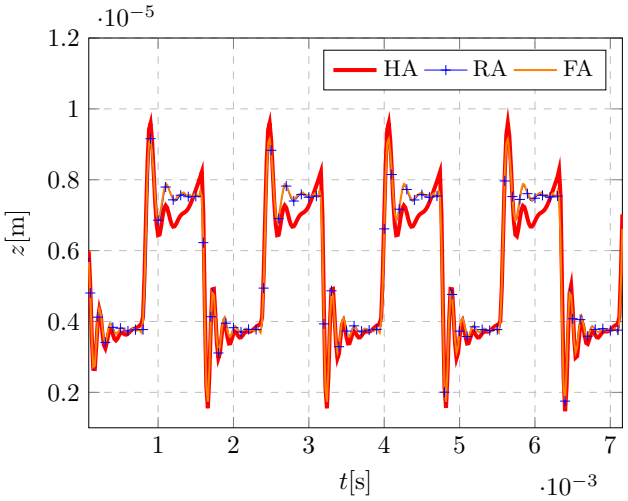

Fig. 4. Vibration displacement in gear mesh system for TVMS models: HA - harmonics approximation, RA - rectangular approximation, FA - Fourier approximation

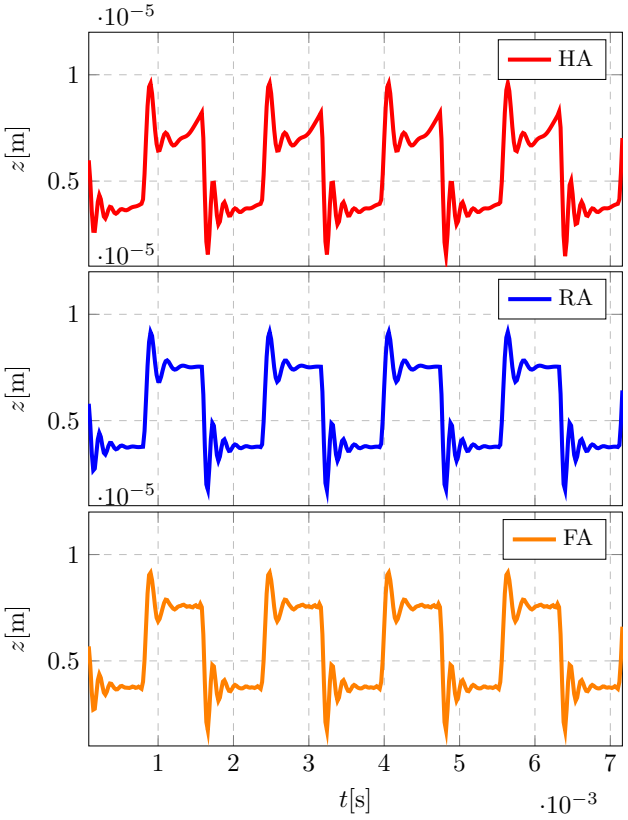

Fig. 5. Vibration displacement in gear mesh system for TVMS models: HA, RA, and FA (subplots from Figure 4)

The RA mesh stiffness signal inherently provides lower accuracy when directly compared with the HA approximation. However, employing a Fourier series expansion in the FA model notably smooths the stiffness variations. Despite this effect, local discrepancies remain, as displacement magnitudes may be artificially exaggerated or diminished at specific time-domain intervals. Furthermore, an intrinsic challenge emerges when using the Fourier series approximation: it

becomes impossible to eliminate artificial mesh stiffness overshoots entirely. These overshoots are attributed to the Gibbs phenomenon, a fundamental feature of Fourier series expansions of periodic functions.

The equivalent force of the inter-tooth interaction can be calculated in the following way (Eq. 27):

$$q_{eq} = \frac{F_c}{m_{eq}} = \frac{c_g \dot{z}}{m_{eq}} + \frac{k_g z}{m_{eq}} \tag{27}$$

where:

q_{eq} - equivalent mesh force;
F_c - mesh force.

The equivalent mesh force (27) can be rearranged to the following form:

$$q_{eq} = \omega_0^2 z + 2h\dot{z} \tag{28}$$

where:

ω_0^2 - natural frequency;
h - damping coefficient.

Figures 6 and 7 show the evolution of dynamic mesh forces and their frequency spectra for the TVMS models, respectively, including damping along the path of contact.

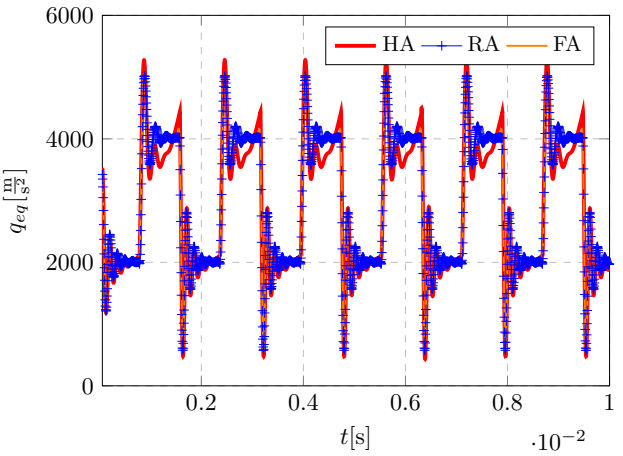

Fig. 6. Dynamic mesh forces along the path-of-contact for TVMS models: HA, RA, and FA

The dynamic effects observed for time-varying equivalent mesh force (Fig. 6) originate primarily from damping phenomena inherent within the gear mesh system. Characteristic changes in the time distribution of the mesh force manifest as periodic variations directly correlated with mesh stiffness (suitable TVMS model) – as depicted in Figure 5.

The mesh force distribution exhibits distinct rapid increases at moments when a single pair of teeth initiates meshing engagement. The gear mesh force attains its peak values at these specific temporal points. Conversely, periods during which two pairs of teeth simultaneously remain meshing within the path of contact are associated with relatively lower force values. This lower mesh force interval extends from entering to exiting the path of contact with a double pair of teeth (during double-tooth meshing until disengagement of one pair). A rapid force's rise recurs as the mesh interaction transitions back to a single-tooth meshing.

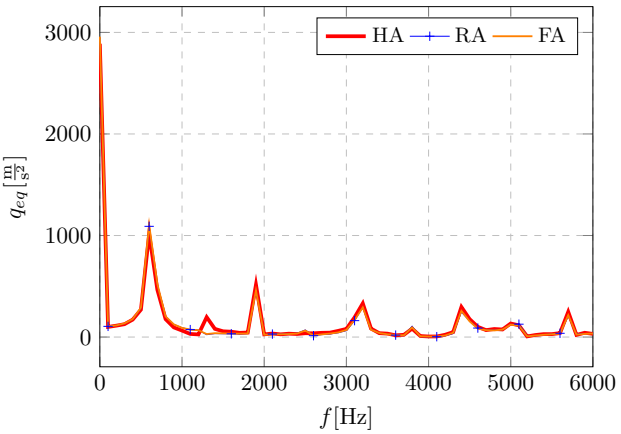

Fig. 7. Frequency spectra of dynamic mesh forces along the path-of-contact for TVMS models: HA, RA, and FA

4. ANALYTICAL SOLUTION

The reduced model (Eq. 29) can be simplified for further analysis [37]. To improve the efficiency of calculations and to avoid multiple executions of complex ones, a computational environment created by the authors is used. This environment is based on the DynPy library and uses Jupyter Notebook, as described above in this paper. The use of the appropriate sequence of methods allows the equation (29) to be determined in a way that is convenient for further analysis. The base code is as follows:

```
dsys = EquivalentSDOFGearModel()

t,z,k,eps=dsys.ivar,dsys.z,dsys.k,dsys.eps
c=dsys.c
F=dsys.F
k_var=dsys.k_var
T=dsys.T
m=dsys.m


delta = Symbol('delta',positive=True)
omg = Symbol('omega',positive=True)
u_s = Symbol('u_s',positive=True)
mu = Symbol('mu',positive=True)

counter=13
data={
    k:counter**2*omg**2,
    c:mu*eps,
    T:2*pi/omg,
    m:1,
    F:counter**2*omg**2*u_s,
    k_var:1,
    omg:1,

msm_ode=gear_dsys.approx_rect(4,numerical=True).
    ode_with_delta().subs(data)
msm_ode
}

    %
```

The code presented allows for a convenient representation of the differential equation in a form ready for perturbation expansion. The result of the execution is as follows:

$$-F + c_g\dot{z} + m_{eq}\ddot{z} + k_g\left(\varepsilon\left(2.27\sin(\omega t) + 0.757\sin(3\omega t)\right) + 1\right)z + \delta k_g\varepsilon z = 0 \tag{29}$$

where:

u_s - static deflection;
δ - detuning parameter;
ω - meshing frequency.

The obtained result represents a recursive system of perturbation equations determined by the Multiple Time Scale Method (MTSM). This problem is solved recursively [43]. It was assumed that the initial system of equations would be the representation of the MTSM system in Jupyter Notebook (graphical representation). The DynPy library allows us to effectively obtain the final solution. The intermediate expressions necessary to obtain the final approximate solution are also possible to analyze. The code responsible for creating the MTSM system is as follows:

```
msm_ode=gear_dsys.approx_rect(4,numerical=True).
    ode_with_delta().subs(data)
msm_ode_subs = msm_ode.odes[0].subs({omg:1,delta
    :delta}).subs({z:(z+u_s)}).subs({}).doit().
    expand()

gear_ode_msm = MultiTimeScaleSolution(
    msm_ode_subs,
                                      ode.dvars
    [0],
                                      ivar=ode.
    ivar, omega=S.One, order=1,eps=eps)

gear_ode_msm

  %
```

The presented code creates an object of the `class MultiTimeScaleSolution`. The result of the code execution is as follow:

$$169z + \mu\varepsilon\dot{z} + 169\delta u_s\varepsilon + 169\delta\varepsilon z + 128.0u_s\varepsilon\sin(3t) + 128.0\varepsilon z\sin(3t) + 384.0u_s\varepsilon\sin(t) + 384.0\varepsilon z\sin(t) + \ddot{z} = 0 \tag{30}$$

where:

u_s - static deflection;
δ - detuning parameter;
ω - meshing frequency.

By calling the corresponding methods on the instance describing the MTSM equation (30), all subsequent solving steps can be obtained. The following executions are possible:

```
gear_ode.predicted_solution_without_scales(3)
gear_ode.predicted_solution(3)

nonlin_ode_base._scales_formula

nth_ord_approx_list = nonlin_ode_base.
    eoms_approximation_list()
nth_ord_approx_list[0]
nth_ord_approx_list[1]

  %
```

The last three executions are responsible for determining the perturbation expansion for the differential equation under consideration (30). They are formed as successive elements of the equation expansion in a power series of the small parameter ε. The zeroth-order and first-order linear approximation (perturbations) have a form of the equations (31) and (32):

$$169z_0(t_0,t_1) + \frac{d^2}{dt_0^2}z_0(t_0,t_1) = 0 \tag{31}$$

$$\begin{aligned} 2\frac{d^2}{dt_1dt_0}z_0(t_0,t_1) + 169z_1(t_0,t_1) + \mu\frac{d}{dt_0}z_0(t_0,t_1) + 169\delta u_s \\ + 169\delta z_0(t_0,t_1) + 128.0u_s\sin(3t_0) \\ + 128.0z_0(t_0,t_1)\sin(3t_0) + 384.0u_s\sin(t_0) \\ + 384.0z_0(t_0,t_1)\sin(t_0) + \frac{d^2}{dt_0^2}z_1(t_0,t_1) = 0 \end{aligned} \tag{32}$$

The environment created during the execution of the work allows for the rapid construction of approximations, as shown by the equations (31) and (32). The obtained results were compared with the reference analytical calculations, confirming the effectiveness of the proposed method [37], and [18], [20], [30], [44]. The differences in the results obtained are due to the different transformation techniques. Finally, the solution (displacements and speed) was determined in the following form:

$$\begin{aligned} z = {} & C_1(t_1)\sin(13t_0) + C_2(t_1)\cos(13t_0) - \delta u_s\varepsilon \\ & + 7.68\varepsilon C_2(t_1)\sin(12t_0) + 0.736\varepsilon C_2(t_1)\sin(16t_0) \\ & + 7.12\varepsilon C_2(t_1)\sin(14t_0) + 0.927\varepsilon C_2(t_1)\sin(10t_0) \\ & - 2.29u_s\varepsilon\sin(t_0) - 7.68\varepsilon C_1(t_1)\cos(12t_0) \\ & - 0.736\varepsilon C_1(t_1)\cos(16t_0) - 0.8u_s\varepsilon\sin(3t_0) \\ & - 7.12\varepsilon C_1(t_1)\cos(14t_0) - 0.927\varepsilon C_1(t_1)\cos(10t_0) \end{aligned} \tag{33}$$

$$C_1(t_1) = \left(C_1\cos\left(\frac{13\delta t\varepsilon}{2}\right) - C_2\sin\left(\frac{13\delta t\varepsilon}{2}\right)\right)e^{-\frac{\mu t\varepsilon}{2}} \tag{34}$$

$$C_2(t_1) = \left(C_1\sin\left(\frac{13\delta t\varepsilon}{2}\right) + C_2\cos\left(\frac{13\delta t\varepsilon}{2}\right)\right)e^{-\frac{\mu t\varepsilon}{2}} \tag{35}$$

where:

C_1, C_2 - integration constants.

$$\begin{aligned} \dot{z} = {} & 13.0C_1(t_1)\cos(13t_0) - 13.0C_2(t_1)\sin(13t_0) \\ & + 11.8\varepsilon C_1(t_1)\sin(16t_0) + 11.8\varepsilon C_2(t_1)\cos(16t_0) \\ & + 9.28\varepsilon C_1(t_1)\sin(10t_0) + 9.28\varepsilon C_2(t_1)\cos(10t_0) \\ & + 92.2\varepsilon C_1(t_1)\sin(12t_0) + 92.2\varepsilon C_2(t_1)\cos(12t_0) \\ & + 99.6\varepsilon C_1(t_1)\sin(14t_0) + 99.6\varepsilon C_2(t_1)\cos(14t_0) \\ & - 2.29u_s\varepsilon\cos(t_0) - 2.4u_s\varepsilon\cos(3t_0) \end{aligned} \tag{36}$$

The received results are consistent with the current state of the art [37]. They differ mainly in the form of the integration constants. This is a very complex expression, and its manual analysis is difficult. The code used facilitates the solution of the computational problem. The obtained results are consistent with similar publications that treat problems of analytical investigation of parametric vibration considering the time-variable mesh stiffness. The proposed methodology, based on object-oriented programming, makes the problem computationally efficient and improves the quick obtaining results. The time complexity of the calculations decreases, reducing the computational cost.

5. MODEL'S SENSITIVITY ANALYSIS TO CHANGES IN MESH PARAMETERS

5.1. Calculation environment for analysis

A sensitivity analysis was carried out to analyze the gear dynamics in more detail and to obtain reference data. A numerical system of motion equations was developed using the dynamic models implemented in the work. The LSODA algorithm provided by the SciPy library [45] was chosen for the simulation. The used environment is based on the Python programming language, which increases computing performance. This allows each solution to be efficiently implemented within the basic programming structures. For this purpose, a procedure to automate the execution of the sensitivity analysis for the selected parameter was written. This procedure code is as follows:

```
1
2  k_values=[3*10**8,6*10**8,9*10**8,1*10**9]
3  c_values=[3*10**3,6*10**3,3*10**4,6*10**4]
4  m_values=[.3,.6,1,2]
5
6  def perform_sensitivity_analysis(param,
       param_span,name,t_span,reference_data):
7
8      data_dict_param = {**reference_data,param:
       param}
9
10     na_df3 = dyn_sys.subs(data_dict_param)(name)
       .numerical_analysis(parameter=param,
       coordinates=2,
11
                           t_span=t_span,
12
                           param_span=param_span
13
                       )
14     results = na_df3.perform_simulations(backend
       ='numpy')
15
16     return results
17
18   %
```

The prepared environment allows for numerical simulations for any shape of the TVMS approximation function. It was decided to carry out simulations with a parabolic TVMS signal to compare the effectiveness of the proposed solution with the results of the research presented in the paper [37], where simulations based on the Fourier approximation of the rectangular TVMS signal were carried out.

[H]

Table 2. Reference values of the parameters for simulations

	Symbol	Value	Unit
Stiffness	k_g	8.0e+8	N/m
Force	F	4.0e+3	N
Damping	c_g	9.0e+3	Ns/m
Period	T	0.0016	s
Mass	m_{eq}	0.57	kg
Small parameter	ε	0.13	-

Using the capabilities of the created environment, a preliminary comparison of the displacements z, velocities $\dot{z}$, and accelerations $\ddot{z}$ during the simulation (gear operation) was made. The results obtained in the time-domain (Figures 8 to 11) and the frequency-domain (Figures 12 to 14) allowed us to select the most interesting simulation results. The reference values of the system's parameters are contained in Table 2.

5.2. Effect of mesh stiffness, k_g

The numerical investigation of these approximated analytical solutions began with a stiffness analysis. Figure 8 shows the time-varying displacement for four mesh stiffness (k_g) values.

Vibrations displacement based on the time-domain signals in Figures 8 and 9 (as subplots) show that the lower the mesh stiffness, the higher the vibration amplitude. The amplitude variability corresponds directly to the changes in the mesh stiffness, whereby the vibration period remains the same.

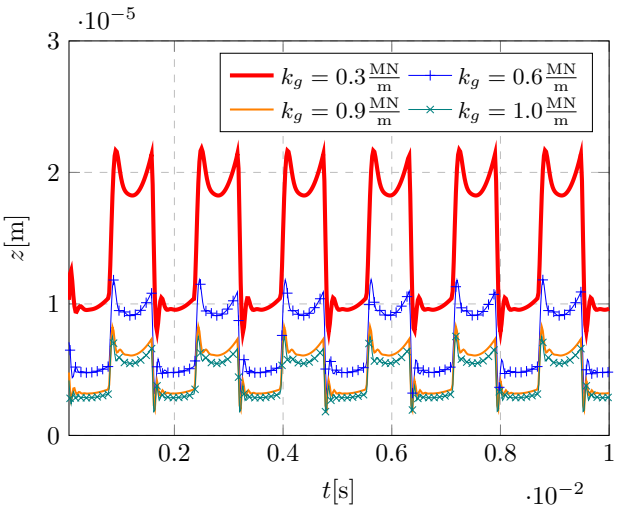

Fig. 8. Time-history of vibration displacement in gear mesh system for selected mesh stiffness coefficients

On the other hand the results in Figure 10 show:

- The signals of velocity in the time domain reveal a more dynamic transient behavior than the displacement, with amplitudes increasing at sudden changes in mesh stiffness.
- At higher mesh stiffness, the speed oscillations decay faster, which means better vibration energy dissipation.

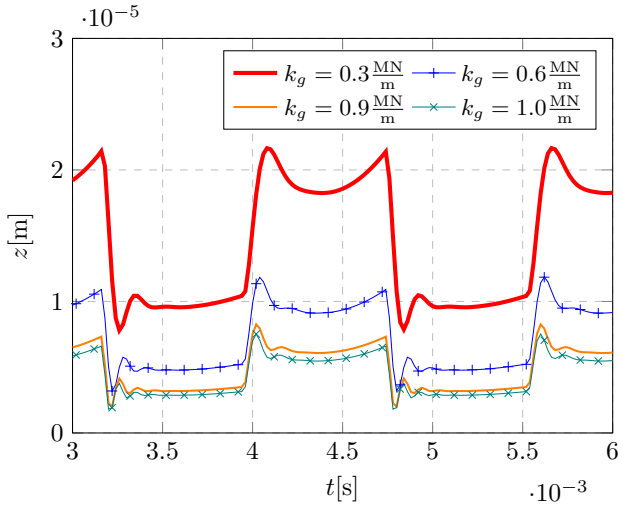

Fig. 9. Time-history of vibration displacement in gear mesh system for selected mesh stiffness coefficients: signals' qualitative zoom from Figure 8 (narrow the time-domain)

- Analysis of the obtained results (presented in the figures) reveals that decrease of the parameter k_g from 0.90 to 0.30 $\frac{\text{N}}{\text{m}}$ results in change of the acceleration level from 3.9E+3 to 5.0E+3 $\frac{\text{m}}{\text{s}^2}$. It means that parameter increases 1.3E+2% (1.3 times)..

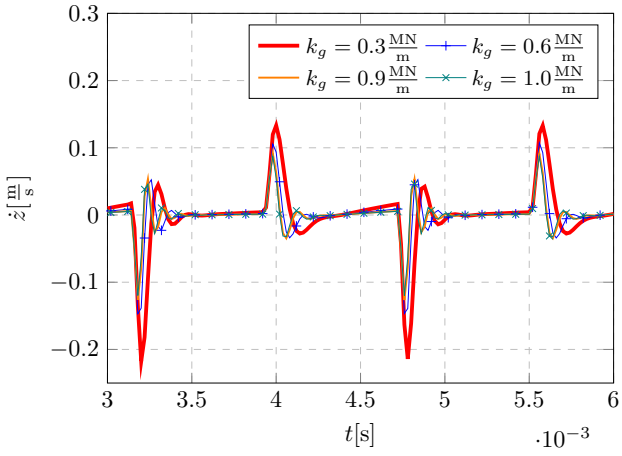

Fig. 10. Time-history of vibration velocity in gear mesh system for selected mesh stiffness coefficients: signals' qualitative zoom (narrow the time-domain)

In turn, an analysis of the results in Figure 11 reveals:

- The acceleration of the vibrations in the time domain maintains constant amplitude values regardless of the mesh stiffness. Still, in transient states, the amplitude increases rapidly, which is related to the constant value of the force loading the gears.
- A particularly clear increase in the acceleration amplitude occurs when switching from single-tooth to double-tooth meshing and vice versa.

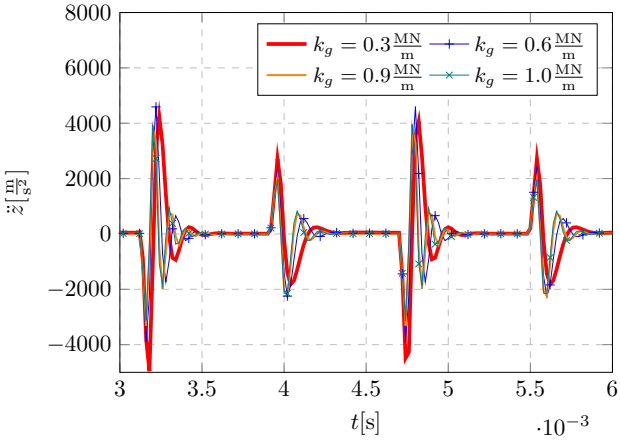

Fig. 11. Time-history of vibration acceleration in gear mesh system for selected mesh stiffness coefficients: signals' qualitative zoom (narrow the time-domain)

The results' analysis allows us to conclude about the higher precision of the analyzed model. The obtained results indicate dynamic behavior consistent with the known results from the literature, which allows us to claim the adequacy of the simplified model described by the selected parameters.

Spectra analysis in Figure 12 indicates:

- The displacement frequency spectrum shows peaks at the gear mesh frequency and its multiples, and an increase in mesh stiffness reduces these values.
- Higher mesh stiffness results in better mechanical stability of the system, limiting the displacement amplitudes.

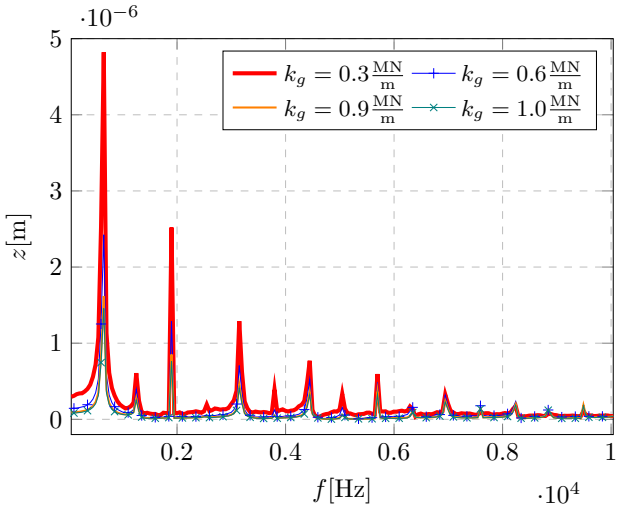

Fig. 12. Frequency spectra of vibration displacement in gear mesh system for selected mesh stiffness coefficients

However, spectral analysis in Figure 13 allows us to conclude that:

- The frequency spectrum of the velocity shows peaks for higher harmonics, and an increase in mesh stiffness causes the energy to be dissipated more quickly over a wider frequency range.

- Higher mesh stiffness improves the dynamic stability of the system, reducing peak velocities and ensuring smoother vibration transitions.

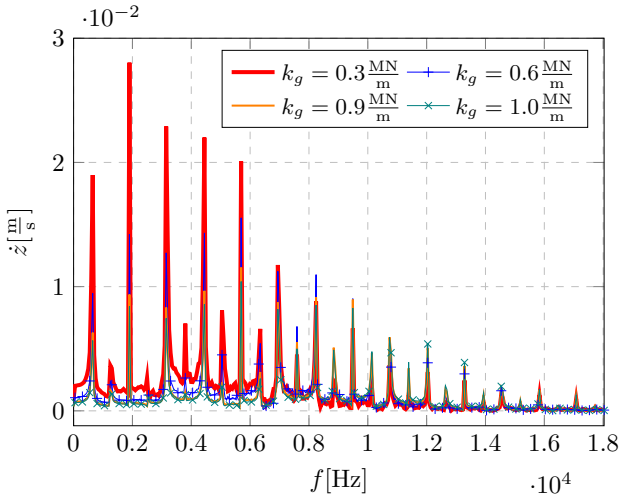

Fig. 13. Frequency spectra of vibration velocity in gear mesh system for selected mesh stiffness coefficients

Figure 14 shows the system's vibration acceleration in the frequency domain. Simulations performed for the parameter k_g allow to observe that if:

- $k_g = 0.30\ \frac{\text{N}}{\text{m}}$ then the highest value (peak) is 667.345 $\frac{\text{m}}{\text{s}^2}$ for $f = 5694.31$ Hz.
- $k_g = 0.60\ \frac{\text{N}}{\text{m}}$ then the highest value (peak) is 518.154 $\frac{\text{m}}{\text{s}^2}$ for $f = 5694.31$ Hz.
- $k_g = 0.90\ \frac{\text{N}}{\text{m}}$ then the highest value (peak) is 423.828 $\frac{\text{m}}{\text{s}^2}$ for $f = 9490.51$ Hz.
- $k_g = 1.0\ \frac{\text{N}}{\text{m}}$ then the highest value (peak) is 392.579 $\frac{\text{m}}{\text{s}^2}$ for $f = 9490.51$ Hz.

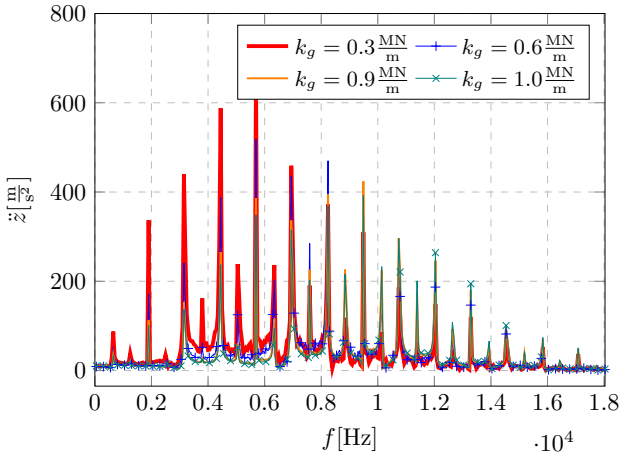

Fig. 14. Frequency spectra of vibration acceleration in gear mesh system for selected mesh stiffness coefficients

Spectra analysis in Figure 14 reveals:

- The acceleration frequency spectrum shows dominant peaks in the meshing frequency, and the higher stiffness causes an increased energy concentration at higher frequencies.
- Higher mesh stiffness reduces peak amplitudes and spreads the energy distribution, which reduces the risk of material fatigue and improves system stability.

General observations show that mesh stiffness has a significant impact on the vibration behavior of the transmission in the drive train. An increase in the mesh stiffness reduces the amplitudes of displacement, velocity, and acceleration, improving vibration stability and limiting the effects of resonance. Transitions between single-tooth and double-tooth meshing generate noticeable peaks in vibration signals, and this effect is more pronounced at lower stiffness.

5.3. *Effect of equivalent mass,* m_{eq}

The next study stage was to identify the impact of the equivalent mass (m_{eq}) of gears on meshing dynamics. The results in Figure 15 allow us to conclude that:

- An increase in the system's mass increases the amplitude of the displacement and changes the frequency of the oscillations, with smaller masses showing greater susceptibility to vibration.
- Higher mass causes a reduction in peak acceleration values and a shift in vibration energy to lower frequencies.
- Investigation of the resultant data (shown in the figures) allows to note that decrease of the quantity m_{eq} from 2.0 to 0.30 kg causes change of the acceleration value from 1.5E+3 to 4.0E+3 $\frac{\text{m}}{\text{s}^2}$. Intepretation of this change states that increases 2.8E+2% (2.8 times)..

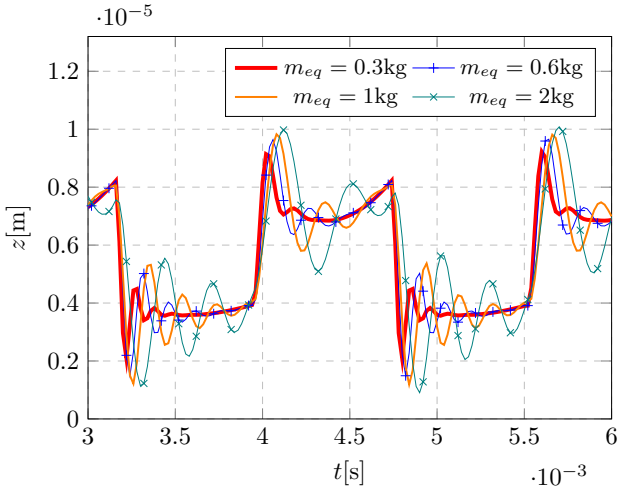

Fig. 15. Time-history of vibration displacement in gear mesh system for selected equivalent mass: signals' qualitative zoom (narrow the time-domain)

An analysis of the time signals (Fig. 15) reveals if the equivalent mass (m_{eq}) increases from 0.3 to 2.0, the amplitude also increases.

Figure 16 shows the system's acceleration response in the frequency domain. Simulations performed for the parameter m_{eq} allow to observe that if:

- $m_{eq} = 0.3$ kg then the highest value (peak) is 443.09 $\frac{\text{m}}{\text{s}^2}$ for $f = 9490.51$ Hz.

- m_{eq} = 0.6 kg then the highest value (peak) is 460.366 $\frac{\text{m}}{\text{s}^2}$ for $f = 5694.31$ Hz.
- m_{eq} = 1 kg then the highest value (peak) is 490.193 $\frac{\text{m}}{\text{s}^2}$ for $f = 5694.31$ Hz.
- m_{eq} = 2 kg then the highest value (peak) is 330.6 $\frac{\text{m}}{\text{s}^2}$ for $f = 3796.2$ Hz.

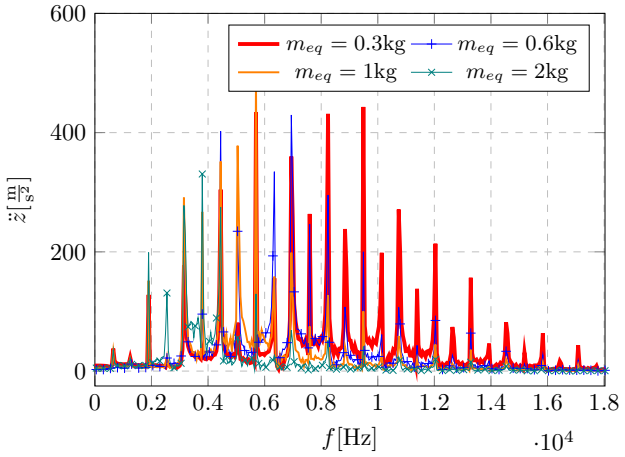

Fig. 16. Frequency spectra of vibration acceleration in gear mesh system for selected equivalent mass

Spectral analysis in Figure 16 shows that for smaller masses ($m_{eq} < 0.6$ kg) the spectrum is more concentrated near the gear mesh frequency. Higher masses (m_{eq} = 1 kg, and more) result in a wider range of observable peaks.

Analysis of the helical gear system for different weights allows specific trends to be observed. The influence of mass on vibration dynamics is important for gear system design. Increasing the mass improves vibration stability by reducing displacements and accelerations, acting as a natural damper. Analysis for specific simulation parameters has shown that the model is inadequate for masses above 3 kg [37].

5.4. Effect of mesh damping, c_g

The graphs in Figure 17 show the system's acceleration response over time for different damping coefficients. The analysis of results shows:

- An increase in the damping ratio reduces the displacement amplitudes, which accelerates the stabilization of the system and reduces oscillations.
- Higher damping values effectively dampen vibrations and dissipate energy faster, stabilizing the system.
- Investigation of the resultant data (shown in the figures) allows to note that decrease of the quantity c_g from 60 to 3.0 $\frac{\text{Ns}}{\text{m}}$ causes change of the acceleration value from 1.2E+3 to 6.6E+3 $\frac{\text{m}}{\text{s}^2}$. Intepretation of this change states that increases 5.4E+2% (5.4 times)..

In a double-tooth meshing, the displacement values are lower, and the number of oscillations increases, whereas in a single-tooth meshing, the damping is less effective. High damping values limit peak amplitudes and dissipate energy over a wider frequency range, reducing the resonance risk.

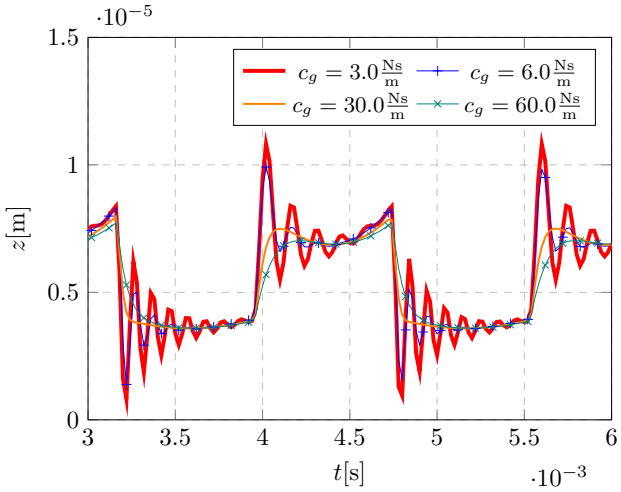

Fig. 17. Time-history of vibration displacement in gear mesh system for selected mesh damping coefficients: signals' qualitative zoom (narrow the time-domain)

In turn, Figure 18 shows the acceleration of the system vibrations in the frequnecy domain for different mesh damping coefficients. Simulations performed for the parameter c_g allow to observe that if:

- c_g = 3.0 $\frac{\text{Ns}}{\text{m}}$ then the highest value (peak) is 979.415 $\frac{\text{m}}{\text{s}^2}$ for $f = 9490.51$ Hz.
- c_g = 6.0 $\frac{\text{Ns}}{\text{m}}$ then the highest value (peak) is 622.249 $\frac{\text{m}}{\text{s}^2}$ for $f = 9490.51$ Hz.
- c_g = 30 $\frac{\text{Ns}}{\text{m}}$ then the highest value (peak) is 192.689 $\frac{\text{m}}{\text{s}^2}$ for $f = 5694.31$ Hz.
- c_g = 60 $\frac{\text{Ns}}{\text{m}}$ then the highest value (peak) is 103.006 $\frac{\text{m}}{\text{s}^2}$ for $f = 5694.31$ Hz.

The shape of the FFT plot remains almost unchaged similarily to stiffness. A behavior of maximal amplitude is observed, where the acceleration decreases for increasing damping. The frequency at which the highest peak appears remains constant except for the extremely high damping value $c_g > 30.0$ $\frac{\text{Ns}}{\text{m}}$.

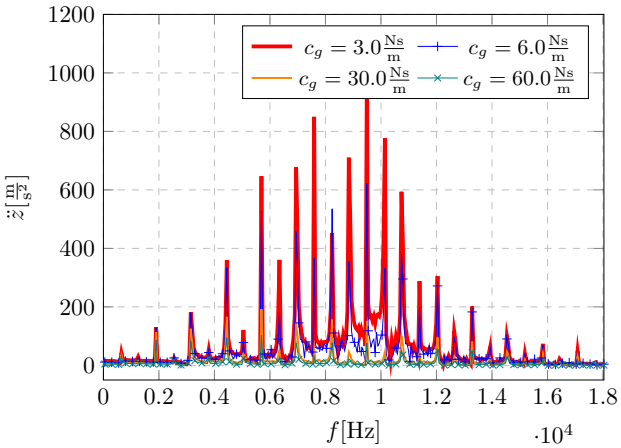

Fig. 18. Frequency spectra of vibration acceleration in gear mesh system for selected mesh damping coefficient

Spectral analysis in Figure 18 allows us to conclude that:

- The highest acceleration peaks occur at low damping coefficients, while an increase in damping reduces the peak values.
- Higher damping disperses energy over a wider frequency range, limiting the risk of resonance and confirming the damping effect (damping efficiency).

Generally, the system's stability increases with the increase of the damping coefficient, minimizing the displacement and acceleration reactions to dynamic loads. Higher damping coefficients cause a rapid decrease in acceleration amplitudes. Effective damping accelerates the reduction of vibration energy, improving the system's work efficiency (system performance) and reducing mechanical fatigue. Optimizing the damping ratio is key to improving machinery's reliability and lifespan.

6. ASSESSMENT OF THE OBTAINED SOLUTION

Assesment of the obtained approximated solution was based on the comparison between numerical approach and analytical results. It allows to show the difference between these methods and possible applications of obtained analytical solution. In order to compare results, the governing equation was transformed to the dimensionless form. It has a following form:

$$\begin{aligned} &169z(\tau)+\mu\varepsilon\frac{d}{d\tau}z(\tau)+169\delta u_s\varepsilon+169\delta\varepsilon z(\tau)\\ &\quad+128.0u_s\varepsilon\sin(3\tau)+128.0\varepsilon z(\tau)\sin(3\tau)\\ &\quad+76.7u_s\varepsilon\sin(5\tau)+76.7\varepsilon z(\tau)\sin(5\tau)\\ &\quad+384.0u_s\varepsilon\sin(\tau)+384.0\varepsilon z(\tau)\sin(\tau)\\ &\quad+54.7u_s\varepsilon\sin(7\tau)+54.7\varepsilon z(\tau)\sin(7\tau)+\frac{d^2}{d\tau^2}z(\tau)=\\ &0 \end{aligned} \tag{37}$$

Obtained equation was solved in the way presented in the previous section and calculated for selected timestamps. A time-domain analysis was performed first, and the results are shown in Figures 19 and 20.

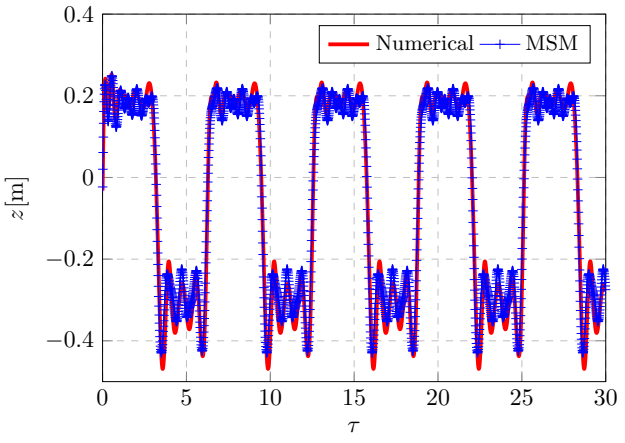

Fig. 19. Comparison of numerical and analytical solution for exemplary data

The comparison between the numerical and analytical solutions demonstrates acceptable differences in the system's displacements. These discrepancies can be attributed to the assume order of approximated solution. The acceptable error margin below 5% (from maximal displacemnts comparison) is visible, however qualitative convergence is better. To confirm this statement, frequency domain analysis was done. The frequency spectrum is presented in Figures 21 and 22.

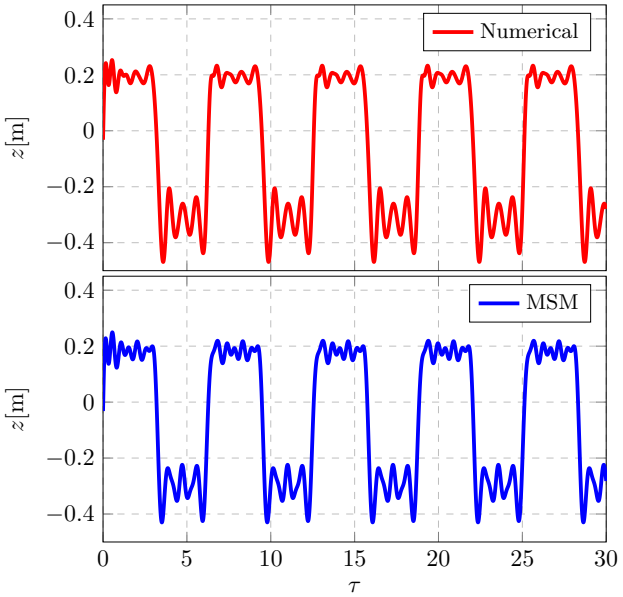

Fig. 20. Comparison of numerical and analytical solution for exemplary data (subplots)

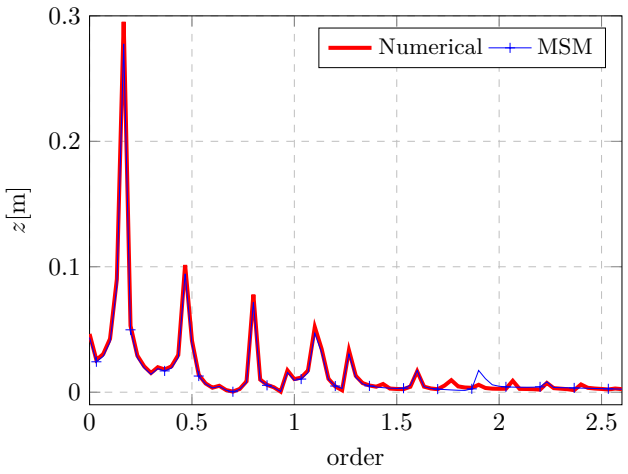

Fig. 21. Comparison of spectral analysis of numerical and analytical solution for exemplary data

The results obtained confirm the convergence of the analytical approach. It is visible that quantitative errors are related to missing harmonical components that are caused by the assumed accuracy of prediction (attribute of perturbational approach). For small values of the parameter ε, the results from both methods are nearly identical, with only minor discrepancies. Obtained results were used to get computation error. The

following formula was used:

$$\Delta = \frac{A_{f1}^{ana} - A_{f1}^{num}}{A_{f1}^{num}} \tag{38}$$

Calcuated erros is aproximatelly 6% for this assesment method, what is more reliable than maximal displacements comparison.

However, as ε increases, the differences between the two methods become more noticeable. These discrepancies manifest as a phase shift between the solutions, with the magnitude of the phase shift and the overall solution difference increasing as ε grows. This behavior highlights the limitations of the multi-scale method for larger perturbations, where higher-order effects cannot be neglected.

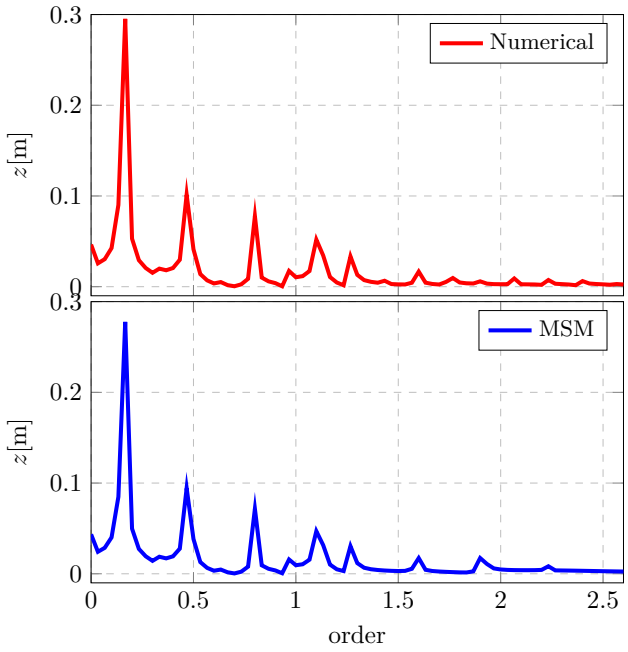

Fig. 22. Comparison of spectral analysis of numerical and analytical solution for exemplary data (subplots)

Overall, the analysis confirms the accuracy of the multi-scale method for small perturbations while emphasizing the need for caution when extending its use to larger values of ε.

7. CONCLUSIONS

The application of the Multiple Time Scales Method (MTSM) to model Time-Varying Mesh Stiffness (TVMS) fills pivotal gaps in the parametric vibration analysis. The main objective was to develop and verify analytical solutions and understand the frequency structure of the meshing phenomenon.

Drawing upon simulations of the helical gear system with TVMS and a comparison of analytical and numerical results, the following conclusions emerge:

1. The proposed two-degree-of-freedom model can be effectively reduced to a one-degree-of-freedom TVMS model and effectively simulates the system's behavior.
2. The proposed approach to applying spectral decomposition results ensures high convergence in the analysis of stiffness characteristics and dynamic response.
3. Minor phase shifts (due to Fourier approximation) limit precision for specific applications, such as control purposes.
4. Despite the complexity of the resulting expressions, these solutions provide valuable insight into system periodicity and amplitude modulation, supporting the overall assessment of meshing dynamics.
5. It should be noted that the analytical solution guarantees the reliability and repeatability of the results due to its explicit mathematical form. This has a direct impact on reducing the computation time.
6. The analytical solution converges with the numerical solution for the second approximation and the value of the small parameter $\varepsilon < 0.1$. Using the first approximation or the value of the small parameter $\varepsilon > 0.1$ results in a marked increase in divergence.
7. The computational framework developed for this study significantly supports the search for an analytical solution using multiple time scales by specialized methods implemented. It fills a gap in currently existing solutions.

Overall, MTSM offers a robust analytical foundation for predicting and managing parametric vibrations in gear systems. Enhancing mesh stiffness and optimising damping improves stability, reduces oscillations, and supports gear durability. These analytical insights can be instrumental in refining helical gear design, enabling early fault detection, vibration minimisation, and more sustainable, operator-friendly machinery performance.

ACKNOWLEDGMENTS

The article was co-financed from the state budget of Poland and awarded by the Minister of Science within the framework of the Excellent Science II Programme

APPENDIX

The code describing dynamic systems is following:

```
class EquivalentGearModel(ComposedSystem):
 """Ready to use sample Single Degree of
 Freedom System with mass on spring
 Arguments:
 =========
     m = Mass
         -Mass of system on spring

     k = Spring coefficient
         -Spring carrying the system

     ivar = symbol object
         -Independant time variable

     qs = dynamicsymbol object
         -Generalized coordinates

 Example
 =======
 A mass oscillating up and down while being
 held up by a spring with a spring constant k
```

```
    >>> t = symbols('t')
    >>> m, k = symbols('m, k')
    >>> qs = dynamicsymbols('z') # Generalized
    Coordinates
    >>> mass = SDoFHarmonicOscillator(m,k, qs=[z
    ],) # Initialization of
    LagrangesDynamicSystem instance

    -We define the symbols and dynamicsymbols
    -Kinetic energy T and potential energy v are
     evaluated to calculate the lagrangian L
    -Reference frame was created with point P
    defining the position and the velocity
    determined on the z axis
    -external forces assigned
    -Next we determine the instance of the
    system using class LagrangeDynamicSystem
    -We call out the instance of the class
    -If necessary assign values for the default
    arguments


    """

    scheme_name = "engine.png"
    real_name = "engine_real.PNG"

    m = Symbol("m_{eq}", positive=True)
    k = Symbol("k_g", positive=True)
    F = Symbol("F", positive=True)
    c = Symbol("c_g", positive=True)
    T = Symbol("T", positive=True)
    omega = Symbol("omega", positive=True)
    ivar = Symbol("t")
    k_var = Symbol("kappa_mesh", positive=True)
    eps = Symbol("varepsilon", positive=True)
    c_var = Symbol("c_var", positive=True)
    f = Symbol("f", positive=True)

    z = dynamicsymbols("z")

    def __init__(
        self,
        m=None,
        k=None,
        F=None,
        z=None,
        c=None,
        T=None,
        ivar=None,
        k_var=None,
        eps=None,
        c_var=None,
        f=None,
        **kwargs,
    ):

        if k_var is not None:
            self.k_var = k_var
        if eps is not None:
            self.eps = eps
        if m is not None:
            self.m = m
        if k is not None:
            self.k = k
        if F is not None:
            self.F = F
        if z is not None:
            self.z = z
        if c is not None:
            self.c = c
        if T is not None:
            self.T = T
        if c_var is not None:
            self.c_var = c_var
        if ivar is not None:
            self.ivar = ivar
        if f is not None:
            self.f = f

        self.qs = [self.z]
        self._init_from_components(**kwargs)

    @cached_property
    def components(self):

        components = {}
        self.c_var = self.c * (1 + 0 * self.eps
    * self.k_var)
        stiffness = self.k * (1 + self.eps *
    self.k_var)

        self.gear_inertia = MaterialPoint(self.m
    , self.z, qs=self.qs)
        self.gear_stiffness = Spring(stiffness,
    self.z, qs=self.qs)
        self.force = Force(self.F, self.z, qs=
    self.qs)
        self.gear_damping = Damper(self.c_var,
    self.z, qs=self.qs)

        components["gear_inertia"] = self.
    gear_inertia
        components["gear_stiffness"] = self.
    gear_stiffness
        components["force"] = self.force
        components["gear_damping"] = self.
    gear_damping

        return components

    def symbols_description(self):
        self.sym_desc_dict = {
            self.m: r"mass of the system on
    spring",
            self.F: r"excitation force",
            self.c: r"damping constant",
            self.k: r"stiffness",
            self.T: r"torque [not sure]",
        }

        return self.sym_desc_dict

    def _report_components(self):

        comp_list = [*REPORT_COMPONENTS_LIST]

        return comp_list

    def units(self):
        f = Symbol("f")
        units_dict = {
            self.k: ureg.newton / ureg.meter,
            self.m: ureg.kilogram,
            self.F: ureg.newton,
            self.ivar: ureg.second,
            self.T: ureg.newton * ureg.meter,
            self.z.diff(self.ivar, 2): ureg.
    meter / ureg.second**2,
            self.c: ureg.newton * ureg.second /
    ureg.meter,
            self.f: ureg.hertz,
```

```
        }
        return units_dict

    def get_numerical_data(self):

        k, m, c, F, eps = symbols("k m c F epsilon", positive=True)

        default_data_dict = {
            self.k: [1e6],
            self.m: [1],
            self.c: [2e-4 * 1e6],
            self.F: [100],
            self.eps: [0.1],
        }
        return default_data_dict

    def trig_stiff(self, angle=2 * pi):
        trig = sin(self.omega * self.ivar)
        new_eq = self.subs(self.k_var, trig)

        return new_eq

    def wave_stiff(self):
        wave1 = (100 * (sin(self.ivar / self.T)) + 1000) * Heaviside(
            sin(self.ivar / self.T)
        )
        wave2 = (100 * (-sin(self.ivar / self.T)) * Heaviside(-sin(self.ivar / self.T))
        waves = wave1 + wave2
        new_eq = self.subs(self.k_var, waves)

        return new_eq

    def rect_stiff(self, no=6, numerical=False):
        t = self.ivar
        omg = self.omega

        trig = sum(
            [Heaviside(omg * t - 1) + 0 * Heaviside(omg * t - 2) for ind in range(no)]
        )
        new_eq = self.subs(self.k_var, trig)

        return new_eq

    def approx_rect(self, no=6, numerical=False):

        if numerical is True:
            amps_list = [
                2.27348466531425,
                0,
                0.757408805199249,
                0,
                0.453942816897038,
                0,
                0.323708002807428,
                0,
                0.25121830779797,
                0,
                0.204977919963796,
                0,
                0.172873394602606,
                0,
                0.149252079729775,
                0,
                0.131121653619234,
                0,
                0.116749954968057,
                0,
            ]
        else:
            amps_list = symbols(f"a_0:{no}")

        rectangular_approx = sum(
            [
                N(amp, 3) * sin(((ind) + 1) * self.omega * self.ivar)
                for ind, amp in enumerate(amps_list[0:no])
            ]
        )
        new_eq = self.subs({self.k_var: (rectangular_approx)})

        return new_eq

    def ode_with_delta(self):
        delta = Symbol("delta", positive=True)
        eps = Symbol("varepsilon", positive=True)

        with_delta = self._eoms[0] + self.k * eps * delta * self.z
        delta_sys = type(self._ode_system)(
            with_delta, Matrix([self.z]), ivar=self.ivar, ode_order=2
        )

        return delta_sys

    def _stiffness_models(self):

        # wave
        t = self.ivar
        T = self.T

        wave1 = (1 * (sin(2 * pi * t / T)) + 2.0) * (
            1 / 2 + 1 / 2 * sign(sin(2 * pi * t / T))
        )
        wave2 = (1 * (-sin(2 * pi * t / T)) - 3.0) * (
            1 / 2 + 1 / 2 * sign(-sin(2 * pi * t / T))
        )
        waves = wave1 + wave2

        # rectangular
        rectangular = 5 * ((1 / 2 + 1 / 2 * sign(sin(2 * pi * t / T))) - S.Half)

        # rectangular_approx
        amps_list = [
            2.27348466531425,
            0.757408805199249,
            0.453942816897038,
            0.323708002807428,
            0.25121830779797,
            0.204977919963796,
            0.172873394602606,
            0.149252079729775,
            0.131121653619234,
            0.116749954968057,
        ]
        rectangular_approx = sum(
            [
                amp * 2 / sqrt(2) * sin((2 * (no) + 1) * 2 * pi * t / T)
```

```
                for no, amp in enumerate(amps_list[0:])
            ]
        )

        return {"wave": waves, "rect": rectangular, "approx": rectangular_approx}

    def _stiffness_waveforms(self):

        from sympy import lambdify

        t = self.ivar
        T = self.T

        return {
            label: lambdify((t, T), waveform)
            for label, waveform in self._stiffness_models().items()
        }

%
```

REFERENCES

[1] H. Ma, J. Zeng, R. Feng, X. Pang, and B. Wen, "An improved analytical method for mesh stiffness calculation of spur gears with tip relief," *Mechanism and Machine Theory*, vol. 98, pp. 64–80, 4 2016. [Online]. Available: https://doi.org/10.1016/j.mechmachtheory.2015.11.017

[2] P. M. Marques, J. D. Marafona, R. C. Martins, and J. H. Seabra, "A continuous analytical solution for the load sharing and friction torque of involute spur and helical gears considering a non-uniform line stiffness and line load," *Mechanism and Machine Theory*, vol. 161, p. 104320, 7 2021. [Online]. Available: https://doi.org/10.1016/j.mechmachtheory.2021.104320

[3] J. I. Pedrero, M. Pleguezuelos, and M. B. Sánchez, "Analytical model for meshing stiffness, load sharing, and transmission error for helical gears with profile modification," *Mechanism and Machine Theory*, vol. 185, p. 105340, 7 2023. [Online]. Available: https://doi.org/10.1016/j.mechmachtheory.2023.105340

[4] Y. Li, S. Yuan, W. Wu, X. Song, K. Liu, and C. Lian, "Dynamic analysis of the helical gear transmission system in electric vehicles with a large helix angle," *Machines*, vol. 11, no. 7, p. 696, 7 2023. [Online]. Available: https://doi.org/10.3390/machines11070696

[5] C.-J. Bahk and R. G. Parker, "Analytical solution for the nonlinear dynamics of planetary gears," *Journal of Computational and Nonlinear Dynamics*, vol. 6, no. 2, p. 021007, 10 2010. [Online]. Available: https://doi.org/10.1115/1.4002392

[6] J. Margielewicz, D. Gąska, and G. Wojnar, "Numerical modelling of toothed gear dynamics," *Scientific Journal of Silesian University of Technology. Series Transport*, vol. 97, pp. 105–115, 11 2017. [Online]. Available: https://doi.org/10.20858/sjsutst.2017.97.10

[7] Y.-C. Chen, "Time-varying dynamic analysis for a helical gear pair system with three-dimensional motion due to bearing deformation," *Advances in Mechanical Engineering*, vol. 12, no. 5, p. 1687814020918128, 5 2014. [Online]. Available: https://doi.org/10.1177/1687814020918128

[8] Z. Cao, Z. Chen, and H. Jiang, "Nonlinear dynamics of a spur gear pair with force-dependent mesh stiffness," *Nonlinear Dynamics*, vol. 99, no. 2, pp. 1227–1241, 1 2020. [Online]. Available: https://doi.org/10.1007/s11071-019-05348-0

[9] S. M. Berri, "Gear vibration analysis: An analytical and experimental study," *International Design Engineering Technical Conferences and Computers and Information in Engineering Conference*, vol. Volume 6C: 18th Biennial Conference on Mechanical Vibration and Noise, pp. 3173–3180, 9 2001. [Online]. Available: https://doi.org/10.1115/DETC2001/VIB-21756

[10] A. Fernandez del Rincon, F. Viadero, M. Iglesias, P. García, A. de Juan, and R. Sancibrian, "A model for the study of meshing stiffness in spur gear transmissions," *Mechanism and Machine Theory*, vol. 61, pp. 30–58, 3 2013. [Online]. Available: https://doi.org/10.1016/j.mechmachtheory.2012.10.008

[11] Z. Wan, H. Cao, Y. Zi, W. He, and Y. Chen, "Mesh stiffness calculation using an accumulated integral potential energy method and dynamic analysis of helical gears," *Mechanism and Machine Theory*, vol. 92, pp. 447–463, 10 2015. [Online]. Available: https://doi.org/10.1016/j.mechmachtheory.2015.06.011

[12] H. Nevzat Özgüven and D. Houser, "Mathematical models used in gear dynamics - a review," *Journal of Sound and Vibration*, vol. 121, no. 3, pp. 383–411, 3 1988. [Online]. Available: https://doi.org/10.1016/S0022-460X(88)80365-1

[13] N. Gao, C. Meesap, S. Wang, and D. Zhang, "Parametric vibrations and instabilities of an elliptical gear pair," *Journal of Vibration and Control*, vol. 26, no. 19-20, pp. 1721–1734, 2 2020. [Online]. Available: https://doi.org/10.1177/1077546320902543

[14] K. Chen, H. Ma, L. Che, Z. Li, and B. Wen, "Comparison of meshing characteristics of helical gears with spalling fault using analytical and finite-element methods," *Mechanical Systems and Signal Processing*, vol. 121, pp. 279–298, 4 2019. [Online]. Available: https://doi.org/10.1016/j.ymssp.2018.11.023

[15] Z. Liu, H. Wei, J. Wei, Z. Xu, and Y. Liu, "Parametric modelling of vibration response for high-speed gear transmission system," *International Journal of Mechanical Sciences*, vol. 249, p. 108273, 7 2023. [Online]. Available: https://doi.org/10.1016/j.ijmecsci.2023.108273

[16] F. Choy, Y. Ruan, J. Zakrajsek, F. Oswald, and J. Coy, "Analytical and experimental study of vibrations in a gear transmission," *27th Joint Propulsion Conference, Sacramento, CA, USA, 24 June 1991 - 26 June 1991*, pp. 1–20, 6 1991. [Online]. Available: https://doi.org/10.2514/6.1991-2019

[17] C. I. L. Park, "Transfer matrix of parametric excited system for noise and vibration analyses of helical gear

system," *Journal of Mechanical Science and Technology*, vol. 35, pp. 4889–4896, 10 2021. [Online]. Available: https://doi.org/10.1007/s12206-021-1007-0

[18] C. I. L. Park, "Vibration from a shaft-bearing-plate system due to an axial excitation of helical gears," *Journal of mechanical science and technology*, vol. 20, pp. 2105–2114, 12 2006. [Online]. Available: https://doi.org/10.1007/BF02916327

[19] C. I. L. Park, "Characteristics of noise generated by axial excitation of helical gears in shaft-bearing-plate system," *Journal of Mechanical Science and Technology*, vol. 29, pp. 1571–1579, 4 2015. [Online]. Available: https://doi.org/10.1007/s12206-015-0329-1

[20] Y. Cai and T. Hayashi, "The linear approximated equation of vibration of a pair of spur gears (theory and experiment)," *Journal of Mechanical Design*, vol. 116, no. 2, pp. 558–564, 6 1994. [Online]. Available: https://doi.org/10.1115/1.2919414

[21] P. Folęga, G. Wojnar, R. Burdzik, and Konieczny, "Dynamic model of a harmonic drive in a toothed gear transmission system," *Journal of Vibroengineering*, vol. 16, no. 6, pp. 3096–3104, 9 2014. [Online]. Available: https://www.extrica.com/article/15571

[22] Y. Zeng, J. Zhu, Y. Han, D. Qiu, W. Huang, and M. Xu, "Dynamic modeling and numerical analysis of gear transmission system with localized defects," *Machines*, vol. 13, no. 4, p. 272, 3 2025. [Online]. Available: https://doi.org/10.3390/machines13040272

[23] A. N. Wieczorek, Konieczny, G. Wojnar, R. Wyroba, K. Filipowicz, and M. Kuczaj, "Reduction of dynamic loads in the drive system of mining scraper conveyors through the use of an innovative highly flexible metal coupling," *Eksploatacja i Niezawodność – Maintenance and Reliability*, vol. 26, no. 2, pp. 1–17, 2024. [Online]. Available: https://doi.org/10.17531/ein/181171

[24] M. Kuczaj, A. N. Wieczorek, Konieczny, R. Burdzik, G. Wojnar, K. Filipowicz, and G. Głuszek, "Research on vibroactivity of toothed gears with highly flexible metal clutch under variable load conditions," *Sensors*, vol. 23, no. 1, p. 287, 2023. [Online]. Available: https://doi.org/10.3390/s23010287

[25] G. Wojnar, R. Burdzik, A. N. Wieczorek, and Konieczny, "Multidimensional data interpretation of vibration signals registered in different locations for system condition monitoring of a three-stage gear transmission operating under difficult conditions," *Sensors*, vol. 21, no. 23, p. 7808, 11 2021. [Online]. Available: https://doi.org/10.3390/s21237808

[26] B. Łazarz, G. Wojnar, and P. Czech, "Early fault detection of toothed gear in exploitation conditions (in polish: Wykrywanie wczesnych faz uszkodzeń kół zębatych w warunkach eksploatacyjnych)," *Eksploatacja i Niezawodność – Maintenance and Reliability*, vol. 1, no. 49, pp. 68–77, 2011. [Online]. Available: https://archive.ein.org.pl/2011-01-09

[27] S. Schmidt, R. Zimroz, and P. S. Heyns, "Enhancing gearbox vibration signals under time-varying operating conditions by combining a whitening procedure and a synchronous processing method," *Mechanical Systems and Signal Processing*, vol. 156, p. 107668, 7 2021. [Online]. Available: https://doi.org/10.1016/j.ymssp.2021.107668

[28] R. Kumar, P. Kumar, G. Vashishtha, S. Chauhan, R. Zimroz, S. Kumar, R. Kumar, M. K. Gupta, and N. S. Ross, "Fault identification of direct-shift gearbox using variational mode decomposition and convolutional neural network," *Machines*, vol. 12, no. 7, p. 428, 6 2024. [Online]. Available: https://doi.org/10.3390/machines12070428

[29] G. Litak and M. I. Friswell, "Vibration in gear systems," *Chaos, Solitons & Fractals*, vol. 16, no. 5, pp. 795–800, 6 2003. [Online]. Available: https://doi.org/10.1016/S0960-0779(02)00452-6

[30] M. Zajíček and J. Dupal, "Analytical solution of spur gear mesh using linear model," *Mechanism and Machine Theory*, vol. 118, pp. 154–167, 12 2017. [Online]. Available: https://doi.org/10.1016/j.mechmachtheory.2017.08.008

[31] P. Velex and L. Flamand, "Dynamic response of planetary trains to mesh parametric excitations," *Journal of Mechanical Design*, vol. 118, no. 1, pp. 7–14, 3 1996. [Online]. Available: https://doi.org/10.1115/1.2826860

[32] K. Feng, J. C. Ji, Q. Ni, and M. Beer, "A review of vibration-based gear wear monitoring and prediction techniques," *Mechanical Systems and Signal Processing*, vol. 182, p. 109605, 1 2023. [Online]. Available: https://doi.org/10.1016/j.ymssp.2022.109605

[33] T. Aihara and K. Sakamoto, "Theoretical analysis of nonlinear vibration characteristics of gear pair with shafts," *Theoretical and Applied Mechanics Letters*, vol. 12, no. 2, p. 100324, 2 2022. [Online]. Available: https://doi.org/10.1016/j.taml.2022.100324

[34] D. Zhang and S. Wang, "Parametric vibration of split gears induced by time-varying mesh stiffness," *Proceedings of the Institution of Mechanical Engineers, Part C: Journal of Mechanical Engineering Science*, vol. 229, no. 1, pp. 18–25, 4 2014. [Online]. Available: https://doi.org/10.1177/0954406214531748

[35] DynPy, "Github: bogumilchilinski/dynpy," 2025-10-12 current version. [Online]. Available: https://github.com/bogumilchilinski/dynpy

[36] B. Chiliński, R. Kwiatkowski, K. Twardoch, and A. Mackojć, "An innovative pendulum-based absorber exploiting time-varying mass dynamics for vibration damping," *Bulletin of the Polish Academy of Sciences Technical Sciences*, vol. 73, no. 5, p. e154285, 7 2025. [Online]. Available: https://doi.org/10.24425/bpasts.2025.154285

[37] K. Twardoch and D. Sierociński, "An analytical approach to gear mesh dynamics for the sustainable design of agricultural machinery drive systems," *Sustainability*, vol. 17, no. 5, p. 1837, 2 2025. [Online]. Available: https://doi.org/10.3390/su17051837

[38] K. Twardoch, K. Górski, R. Kwiatkowski,

K. Jaśkielewicz, and B. Chiliński, "Adaptive pendulum-tuned mass damper based on adjustable-length cable for skyscraper vibration control," *Sustainability*, vol. 17, no. 14, p. 6301, 7 2025. [Online]. Available: https://doi.org/10.3390/su17146301

[39] D. Sierociński, B. Chiliński, F. Gawiński, A. Radomski, and P. Przybyłowicz, "Dynpy—python library for mechanical and electrical engineering: An assessment with coupled electro-mechanical direct current motor model," *Energies*, vol. 18, no. 2, p. 332, 1 2025. [Online]. Available: https://doi.org/10.3390/en18020332

[40] M. Żurawski, B. Chiliński, and R. Zalewski, "A novel method for changing the dynamics of slender elements using sponge particles structures," *Materials*, vol. 13, no. 21, p. 4874, 10 2020. [Online]. Available: https://doi.org/10.3390/ma13214874

[41] M. Żurawski, R. Zalewski, and B. D. Chiliński, "Concept of an adaptive-tuned particles impact damper," *Journal of Theoretical and Applied Mechanics*, vol. 58, no. 3, pp. 811–816, 7 2020. [Online]. Available: https://doi.org/10.15632/jtam-pl/122431

[42] "Sympy: 1.12 released," 2023-05-10. [Online]. Available: https://www.sympy.org/en/index.html

[43] B. Chilinski, A. Mackojc, and K. Mackojc, "Analytical solution of parametrically induced payload nonlinear pendulation in offshore lifting," *Ocean Engineering*, vol. 259, p. 111835, 9 2022. [Online]. Available: https://doi.org/10.1016/j.oceaneng.2022.111835

[44] C.-J. Bahk and R. G. Parker, "Analytical solution for the nonlinear dynamics of planetary gears," *Journal of Computational and Nonlinear Dynamics*, vol. 6, no. 2, p. 021007, 4 2011. [Online]. Available: https://doi.org/10.1115/1.4002392

[45] "Scipy: 1.15.2 released," 2025-02-16. [Online]. Available: https://scipy.org